BNL-96183-2011-CP

Development of CdZnTe Radiation Detectors

A. Bolotnikov, G. Camarda, A. Hossain, K.H. Kim, G. Yang, R. Gul, Y. Cui, and R.B. James

Submitted for Presentation at the 2011 IEEE Nuclear Science Symposium and Medical Imaging Conference (2011 NSS/MIC)
Valencia, Spain
October 23-29, 2011

August 2011

Nonproliferation and National Security Department

Brookhaven National Laboratory

U.S. Department of Energy
Office of Science, National Nuclear Security Administration

Notice: This manuscript has been authored by employees of Brookhaven Science Associates, LLC under Contract No. DE-AC02-98CH10886 with the U.S. Department of Energy. The publisher by accepting the manuscript for publication acknowledges that the United States Government retains a non-exclusive, paid-up, irrevocable, world-wide license to publish or reproduce the published form of this manuscript, or allow others to do so, for United States Government purposes.

This preprint is intended for publication in a journal or proceedings. Since changes may be made before publication, it may not be cited or reproduced without the author's permission.

DISCLAIMER

This report was prepared as an account of work sponsored by an agency of the United States Government. Neither the United States Government nor any agency thereof, nor any of their employees, nor any of their contractors, subcontractors, or their employees, makes any warranty, express or implied, or assumes any legal liability or responsibility for the accuracy, completeness, or any third party's use or the results of such use of any information, apparatus, product, or process disclosed, or represents that its use would not infringe privately owned rights. Reference herein to any specific commercial product, process, or service by trade name, trademark, manufacturer, or otherwise, does not necessarily constitute or imply its endorsement, recommendation, or favoring by the United States Government or any agency thereof or its contractors or subcontractors. The views and opinions of authors expressed herein do not necessarily state or reflect those of the United States Government or any agency thereof.

Development of CdZnTe Radiation Detectors

Aleksey Bolotnikov, Giuseppe Camarda, Anwar Hossain, Ki Hyun Kim, Ge Yang, Rubi Gul,
Yonggang Cui* and Ralph B. James
Brookhaven National Laboratory, Upton, NY, USA

ABSTRACT

Cadmium Zinc Telluride (CdZnTe or CZT) is a very attractive material for room-temperature semiconductor detectors because of its wide band-gap and high atomic number. Despite these advantages, CZT still presents some material limitations and poor hole mobility. In the past decade most of the efforts developing CZT detectors focused on designing different electrode configurations, mainly to minimize the deleterious effect due to the poor hole mobility. A few different electrode geometries were designed and fabricated, such as pixelated anodes and Frisch-grid detectors developed at Brookhaven National Lab (BNL) [1][2]. However, crystal defects in CZT materials still limit the yield of detector-grade crystals, and, in general, dominate the detector's performance. In the past few years, our group's research extended to characterizing the CZT materials at the micro-scale, and to correlating crystal defects with the detector's performance. We built a set of unique tools for this purpose, including infrared (IR) transmission microscopy, X-ray micro-scale mapping using synchrotron light source, X-ray transmission- and reflection- topography, current deep level transient spectroscopy (I-DLTS), and photoluminescence measurements. Our most recent work on CZT detectors was directed towards detailing various crystal defects, studying the internal electrical field, and delineating the effects of thermal annealing on improving the material properties. In this paper, we report our most recent results.

Keywords: CdZnTe, Radiation detectors, Crystal defects

1. INTRODUCTION

Cadmium Zinc Telluride (CdZnTe or CZT) is a very attractive material for room-temperature semiconductor detectors, because it has a wide band-gap and a high atomic number [3]. Over the past two decades, extensive efforts were made in ameliorating the material's properties toward detector-grade crystals. These fruitful results on crystal growth, post-growth annealing, and device fabrication generated detector-grade crystals up to 2 cm^3, and facilitated the fabrication of CZT-based devices / systems suitable for applications in the fields of nonproliferation, national security, and medical imaging. However, the availability of large-volume CZT detectors remains limited. The presence of various extended defects degrades the detector's performance. Further improvements on growing CZT crystals and fabricating detectors rely upon our gaining better understanding of the correlations between various defects and the detector's performance.

Our group at Brookhaven National Laboratory (BNL) was funded to undertake material characterization and detector testing to address this problem. Our procedure is to assure that we cooperate closely with the vendors of the CZT crystals in specifying their growth conditions. Then, the crystals are characterized by classifying the various extended defects. Thereafter, we fabricate CZT detectors from intriguing regions in the wafers, and their spectral performance is tested. From the results generated we can address the correlations between the extended defects and the detector's performance. Then, the output from our research is fed back to the vendors to modify and improve the crystal's growth process.

The techniques that we are using include infrared (IR) transmission microscopy and several unique tools at BNL's National Synchrotron Light Source (NSLS), i.e., Micron-scale X-ray Detector Mapping (MXDM) and White-Beam X-ray Diffraction Topography (WBXDT). To understand the influence of post-growth annealing on extended defects, we also conduct thermal annealing experiments on selected CZT samples. Our recent findings revealed charge trapping at Te inclusion sites and sub-grain boundaries. In addition we also demonstrated that individual dislocations are less important than other defects in determining the performance of CZT detectors. In the following sections, we will discuss the details of these techniques and report the test findings.

* ycui@bnl.gov; phone 1 631 344-5351; fax 1 631 344-876; www.bnl.gov

2. EXPERIMENTAL TECHNIQUES

2.1 Infrared (IR) Transmission Microscopy

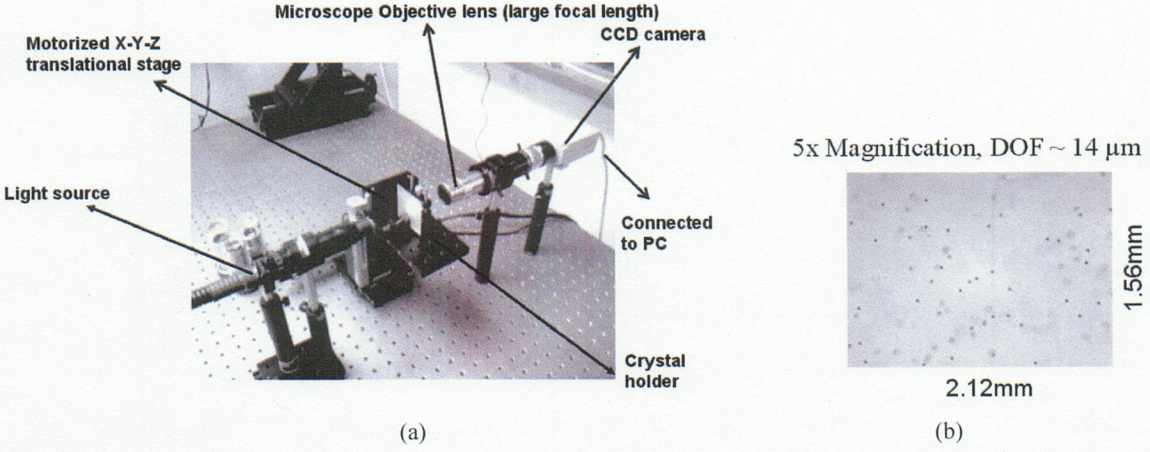

Figure 1. (a) IR transmission microscope imaging system; (b) A typical IR transmission image of a CZT sample showing Te inclusions in the bulk.

CZT crystals are transparent to the IR light, but Te inclusions are opaque. We established an automatic IR microscopy system to examine the Te inclusions in the bulk of CZT materials [4]. Figure 1 (a) illustrates the setup of the imaging system. The IR light generated from a light source (not shown in the photo) is transmitted on the CZT sample via a fiber-optic guide and a condensator. A CCD camera, installed on the other side of the sample, has an imaging sensor of 2208x3000 pixels; each pixel is 3.5x3.5 μm^2. When coupled to microscope objective lens with magnification larger than five, the system provides sub-micron spatial resolution. A computer program controls the motorized X-Y-Z translational stage on which the CZT sample sits, allowing us to focus on different depths at different regions of the sample; images are acquired at each depth. In addition, the software also contains a histogram function to control the images' brightness. A typical IR image of CZT sample in Figure 1 (b) reveals Te inclusions decorating the bulk of the crystal. In addition to taking a single shot, the software can acquire a series of images within a predefined field of view (FOV) and depth boundaries.

2.2 Micron-scale X-ray Detector Mapping

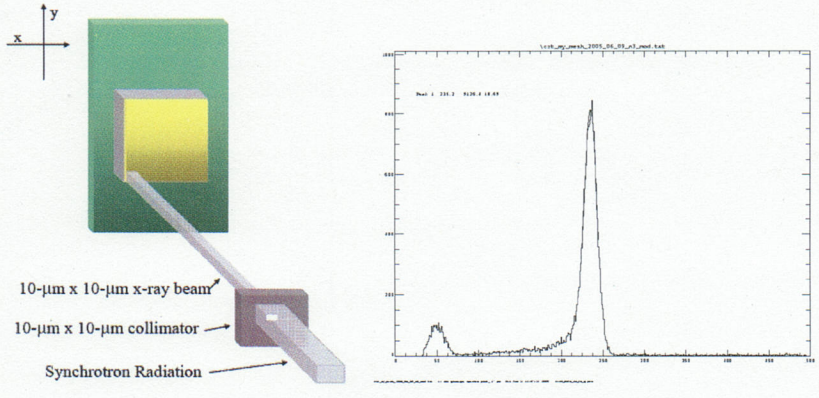

Figure 2. (a) Setup of Micron-scale X-ray Detector Mapping system; (b) Measured spectral response of a CZT detector with the X-ray beam targeting a specific area on the sample.

Micron-scale X-ray Detector Mapping is a unique technique that we developed at BNL's National Synchrotron Radiation Source (NSLS). With this technique (Figure 2), we can deliver a fine collimated X-ray beam (10×10 μm^2), ranging from 7 keV to 40 keV, on to a specific area of a CZT detector. Using a hybrid charge-sensitive amplifier followed by a shaping circuit and multi-channel analyzer (MCA), we can measure the spectral response in that specific area and extract the associated information, i.e., pulse height, photopeak position, and FWHM. With our software, we can do a raster scan to control the translation stages and move the sample in the x- and y-directions. Hence, we can map the detector's energy response (normally denoted by the photopeak's position) over the entire detection area. Since the X-ray beam is very tiny, we can study how a localized defect affects the detector's performance. This unique test cannot be done easily with a sealed radioactive source because, after fine collimation, its X- or gamma- ray intensity is extremely low, and testing takes many days or months. However, with the bright, highly collimated X-ray at the NSLS, testing is rapid and easy. It takes only a few seconds to finish a test at one beam position, and a few hours (depending on the beam's size and the detector's size) to scan an entire detector.

2.3 White Beam X-ray Diffraction Topography (WBXDT)

White Beam X-ray Diffraction Topography (WBXDT) measurements allow us to examine the distribution of defects and strains in CZT crystals. Bragg's Law describes the principles of the operation of WXDT as [4].

$$\lambda = 2d\cdot\sin\theta_B ,$$

where λ is the wavelength of the X-rays, θ_B is the angle between the incident X-rays and the lattice planes of CZT crystal (Figure 3), and d is the interplanar distance between two adjacent lattice planes. From this equation, we know the following: (1) X-ray diffraction measures the crystal's lattice-structure, i.e., the topography of the lattice planes around the defects, and (2) as the lattice structure around the defects changes, the incident angle θ_B changes, weakening the intensity of diffracted X-ray in the direction of diffraction of perfect lattice plane. The intensity variation on the image reveals detailed information about the defects; and, (3) when we use white-beam X-ray, multiple diffraction images form because the beam is composed of X-rays with different wavelengths, so allowing us to select the images with high contrast for further analysis.

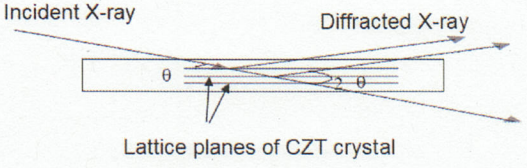

Figure 3. WXDT experiment.

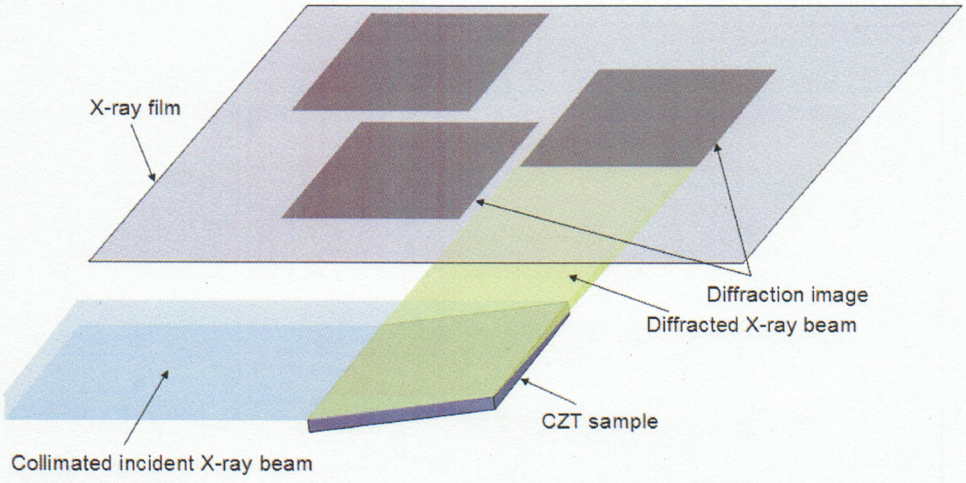

Figure 4. Sketch of the experimental WBXDT setup.

Figure 4 shows the sketch of the WBXDT experimental setup. The input X-ray beam covers the entire sample area under study; this avoids unnecessary scattering if using a much larger beam than the sample being tested. The CZT, installed on a sample holder controlled by translation stages, is tilted slightly with its top surface exposed to the incident X-ray beam. An image plate, installed above the CZT sample, records the diffraction images. Depending on the orientation of the crystal, the incident X-ray beam is diffracted along multiple directions, forming multiple diffraction images as shown in the figure. In addition, if the crystal has multiple domains, each domain will have specific reflection directions, and the images will have irregular shapes representing the domain's shape.

3. HIGHLIGHTS OF RECENT RESEARCH RESULTS

3.1 Charge Trapping by Te inclusions

Figure 5 (a) shows the mapping of peak positions during the raster scan over a detector's active area. The darker spots corresponding to the lower peak-positions are due to incomplete charge-collection in that area. Comparing this image with the IR image of the same sample (Figure 5 (b)), clearly reveals the one-to-one correlation between the low efficiency area in the X-ray response map and the Te inclusions in the IR map, proving that the X-ray mapping technique is a unique, powerful tool for studying defects in CZT material. We also explored this charge-trapping effect quantitatively by plotting the X-ray mapping in a 3D view (Figure 5 (c)) in custom software written and described by Bolotnikov et al. [5][6]. Based on experimental results, we constructed a model to simulate the physics of the trapping effect. The effect caused by Te inclusions of different sizes is illustrated in Figure 5 (d) [7]. The findings show that, for concentration of Te inclusions below 10^5 cm^{-3}, only Te inclusions larger than ~3 μm degrade the CZT detectors' spectral performance very much; the effect of smaller inclusions can be neglected [7]. This result from the simulation agrees with that from the calculation in [8].

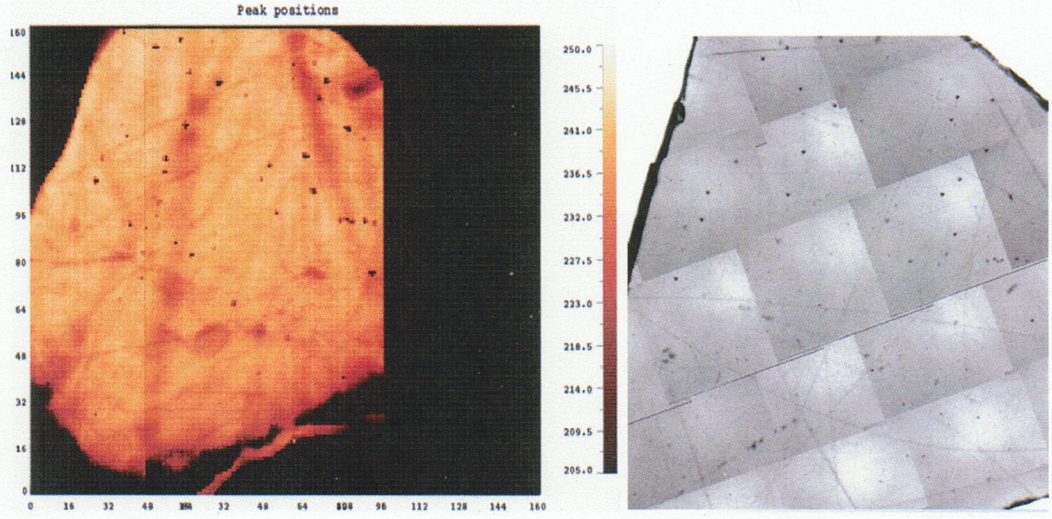

(a) (b)

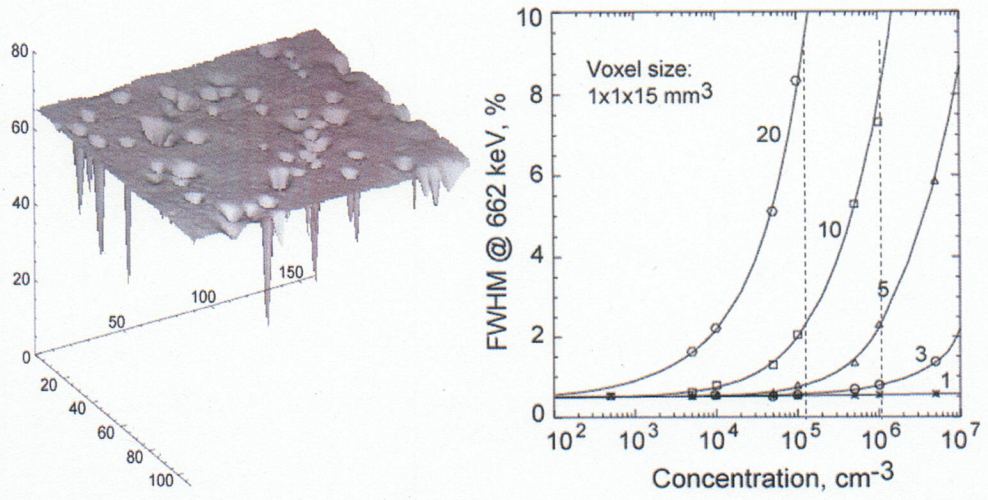

Figure 5. Micron-scale X-ray Detector Mapping shows the Te inclusions and their charge-trapping effect. (a) 2D X-ray response map. The darker spots represent low charge-collection efficiency regions; (b) IR image of the same sample showing the Te inclusions that have a one-to-one correlation with the darker spots in (a); (c) 3D view of the X-ray response map showing the regions with degraded charge-collection efficiency; and, (d) Simulation results of the charge-trapping effect of Te inclusions of different sizes. [7]

3.2 Influence of Dislocation-related Defects on the Detector's Performance

In addition to Te inclusions, other defects occur in CZT crystals, such as twins, sub-grain boundaries, and dislocations. Most of them are transparent to IR light unless Te inclusions decorate them. Consequently, vendors cannot see these defects by simply examining the samples under an IR microscope (available to most of them). However, the presence of these defects may play an important role in determining the detector's performance. In this study, we selected a few CZT samples with specific defect features and measured their spectral response in an X-ray mapping experiment.

Our first test was done on a 2-mm thick detector with cellular structure dislocations; Figure 6 (a) is its X-ray response map. The cellular structure is decorated by Te inclusions. The 3D view of the X-ray response map denotes that such defects trap only a very small amount of charge and cause broadening of the photopeaks in the spectra. This charge loss can be corrected with information on the depth-of-interaction (DOI).

The second test was done on a detector with large-scale grain boundary across the detector. Its X-ray response map is shown in Figure 7(a) [9]. The spectral response (Figure 7(b)) has two photopeaks, indicating that defects along the grain boundary trap a large amount of charge shifting the photo-peak signals [9]. In addition to broadening the photo-peak, the defects also divert some signals away from it and move them to the continuums in the spectra. Such crystals should be avoided in fabricating CZT detectors.

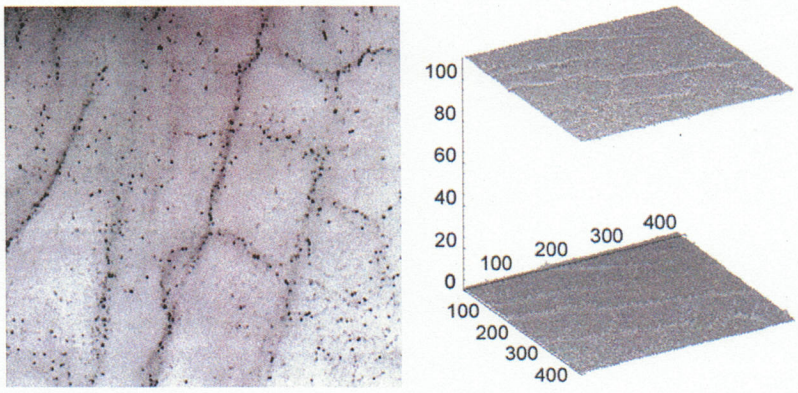

(a) (b)

Figure 6. X-ray response map image of a CZT detector with dislocations distributed in a mosaic structure in the bulk of a CZT crystal. (a) 2D image; (b) 3D view of the same data.

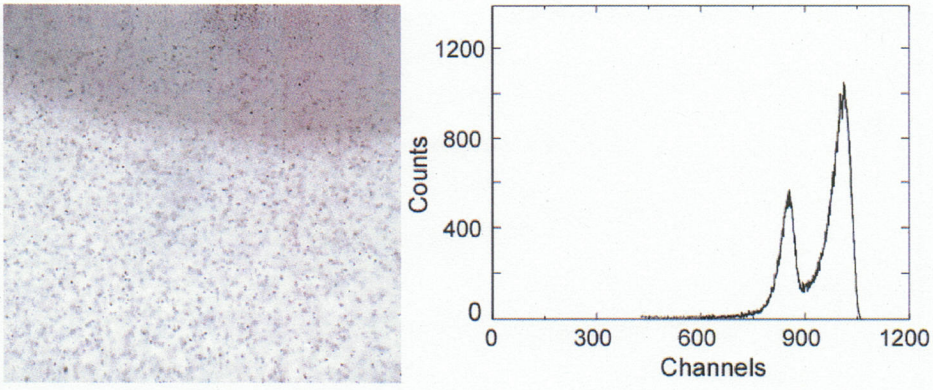

(a) (b)

Figure 7. (a) X-ray response map shows the grain boundary across the CZT sample under test; (b) spectral response of the detector.

3.3 E-field Distortion Caused by Dislocations

For this measurement, we selected two 20x20x2 mm^3 detectors with high resistivity and high $\mu\tau$-product, but impaired with microscopic extended defects, such as cellular structure dislocations and micro-twins. Each detector was pixelated with an array of 32x32 anodes, and its pitch was about 0.625 mm. Figure 8 (a) shows the pattern of electrodes. For this work, we developed a special substrate wherein the pixels are connected diagonally and separated into two groups, one for signal readout and one acting as the short-circuit to ground (Figure 8 (b)). For detectors without defects, the X-ray response map looks like a chessboard. However, our two detectors gave the response images reproduced in Figure 8 (c) and (e); their WBXDT images appear, respectively, in Figure 8 (d) and (f) [10]. From the X-ray response maps, it is apparent that some pixel patterns are enlarged and deformed from their origin square geometry. The only possible reason for this is that the charge generated by the incident X-ray beam had drifted to the adjacent pixels instead of going to the pixel that the beam had targeted. In other words, the local effects, viz., the cellular structure dislocations, distorted the internal E-field. In addition, we noticed a large distortion across the detector corresponding to the sub-grain boundaries in these crystals as seen in the WBXDT images. In some areas, no signal response was detected. This finding indicates that sub-grain boundaries affect the spectral response of CZT detectors in two ways: charge trapping by the Te inclusions decorating the sub-grain boundaries; and, E-field distortion caused by dislocations along the sub-grain boundaries. More detailed discussions were reported in [11].

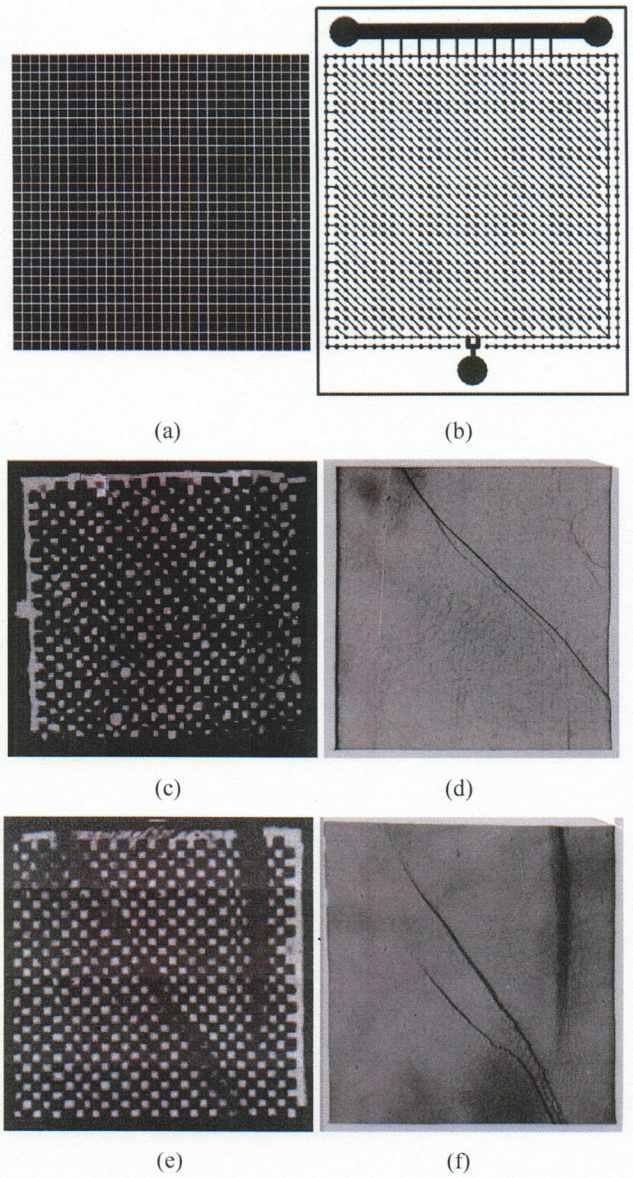

Figure 8. (a) Anode pattern of the two detectors under test; (b) Chessboard connection between pixels on the detector substrate; (c) X-ray response map of detector 1; (d) WBXDT image of detector 1; (e) X-ray response map of detector 2; and, (f) WBXDT image of detector 2.

4. CONCLUSIONS

Employing our suite of unique techniques available at BNL, we investigated the correlations between extended defects and the performance of CZT detectors. Our results show that large (>3 μm) Te inclusions trap the charge and degrade the detectors' spectral response. Sub-grain boundaries are another major defect that lowers the detector performance. In addition to trapping the charge at the dislocation sites along the boundary, they also change the internal E-field distribution inside the detector. We also identified individual dislocation bands identified in the CZT crystals; their effect on detector performance was not as important as was that from Te inclusions and sub-grain boundaries.

5. ACKNOWLEDGEMENT

This work was supported by U.S. Department of Energy, Office of Nonproliferation Research and Development, NA-22, and U.S. Department of Defense, Defense Threat Reduction Agency, DTRA. The manuscript has been authored by Brookhaven Science Associates, LLC under Contract No. DE-AC02-98CH1-886 with the US Department of Energy. The United States Government retains, and the publisher, by accepting the article for publication, acknowledges, a world-wide license to publish or reproduce the published form of this manuscript, or allow others to do so, for the United States Government purposes.

REFERENCES

[1] A. E. Bolotnikov, N. M. Abdul-Jabbar, S. Babalola, G. G. Camarda, Y. Cui, A. Hossain, E. Jackson, H. Jackson, J. R. James, A. L. Luryi, and R. B. James, "Optimization of virtual Frisch-grid CdZnTe detector designs for imaging and spectroscopy of gamma rays", Proceedings of SPIE Conference on Hard X-Ray and Gamma-Ray Detector Physics IX, Vol. 6706, edited by R. B. James, A. Burger, and L. A. Franks, San Diego, CA, pp. 670603-1-13.

[2] A. E. Bolotnikov, G. C. Camarda, G. A. Carini, M. Fiederle, L. Li, D. S. McGregor, W. McNeil, G. W. Wright and R. B. James, "Performance characteristics of Frisch-ring CdZnTe detectors", IEEE Trans. Nucl. Sci., Vol. 53, Issue 2, 2006, pp. 607-614.

[3] T. E. Schlesinger and R. B. James, Semiconductors and Semimetals, in Semiconductors for Room Temperature Nuclear Detector Applications, Vol. 43, San Diego, CA: Academic, 1995.

[4] G. S. Camarda, N. M. Abdul-Jabbar, S. Babalola, A. E. Bolotnikov, Y. Cui, A. Hossain, E. Jackson, H. Jackson, J. R. James, A. L. Luryi, M. Groza, A. Burger, and R. B. James, "Characterization and Measurements of CZT Material: Novel Techniques and Results", Proceedings of SPIE Hard X-Ray and Gamma-Ray Detector Physics IX, Vol. 6706, edited by R. B. James, A. Burger and L. A. Franks, 670605. Nov. 2007.

[5] G. S. Camarda, A. E. Bolotnikov, G. A. Carini, and R. B. James, "Effects of Tellurium Inclusions on charge collection in CZT Nuclear Radiation Detectors", in Countering Nuclear and Radiological Terrorism, edited by S. Aprkyan and D. Diamond, Springer, 2006, pp. 199-207.

[6] G. A. Carini, A. E. Bolotnikov, G. S. Camarda, and R. B. James, "High-resolution X-ray mapping of CdZnTe detectors", Nucl. Instrum. Meth. A 579, 120-124 (2007).

[7] A. E. Bolotnikov, G. S. Camarda, G. A. Carini, Y. Cui, K. T. Kohman, L. Li, M. B. Salomon and R. B. James, "Performance-Limiting Defects in CdZnTe Detectors", IEEE Trans. Nucl. Sci., vol. 54, No. 4, pp. 821-827, 2007.

[8] D. S. Bale, "Homogenization theory for the cumulative effect of Te inclusions in CdZnTe radiation detectors", J. App. Phys., vol. 107, 2010; doi:10.1063/1.3275862.

[9] A. E. Bolotnikov, S. Babalola, G. G. Camarda, Y. Cui, R. Gul, S. U. Egarievwe, P. M. Fochuk, M. Fuerstnau, A. Hossain, F. Jones, K. Kim, O. V. Kopach, L. Carchini, B. Raghothamachar, R. Taggart, G. Yang, L. Xu and R. B. James, "Correlations between crystal defects and performance of CdZnTe detectors", 17th Room Temperature Semiconductor Detector Workshop (invited talk), Knoxville, TN, October, 2010.

[10] G. S. Camardaa, A. E. Bolotnikova, W. Chanc, Y. Cuia, M. Fuerstnaud, P. M. Fochukb, R. Gula, J. Horacec, A. Hossaina, F. Jonese, K. H. Kima, B. McCallc, B. Raghothamacharf, R. Taggarth, A. Wilderc, L. Xua,g, G. Yanga, and R. B. Jamesa, "Study of the internal E-field in planar and pixellated CdZnTe Detectors", 17th Room Temperature Semiconductor Detector Workshop (invited talk), Knoxville, TN, October, 2010.

[11] G. S. Camarda, K. W. Andreini, A. E. Bolotnikov, Y. Cui, A. Hossain, R. Gul, K. H. Kim, L. Marchini, L. Xu, G. Yang, J. E. Tkaczyk and R. B. James, "Effect of extended defects in planar and pixilated CdZnTe detectors", Nucl. Instr. And Meth. In Phys. 2011; doi:10.1016/j.nima.2010.12.012.